

Clustering model in n -doped many-valley semiconductors

M. Fabbri and A. Ferreira da Silva

*Instituto de Pesquisas Espaciais, Conselho Nacional de Desenvolvimento Científico e Tecnológico,
12200 São José dos Campos, São Paulo, Brazil*

(Received 3 October 1983)

We investigate the microscopic structure of the impurity states in n -silicon as an example of randomly distributed donor impurities in a diamond-structure many-valley semiconductor. An improved Hartree-Fock-Roothaan scheme with spin-polarized potentials and Kohn-Luttinger donor wave functions associated with each impurity were used in the calculation. It is shown that the many-valley character of the host gives rise to a distribution of impurity clusters of various sizes, quite different from the case of neglecting the valley multiplicity, and that it strongly reduces the self-compensation effect due to the potential fluctuation. The results are in agreement with recent investigations that have appeared in the literature.

I. INTRODUCTION

Shallow donor-impurity states in semiconductors have attracted much attention, because they provide a typical example which exhibits a metal-nonmetal (MNM) transition at low temperatures as a function of impurity concentration. This MNM transition, which is usually discussed in terms of the Mott-Hubbard-Anderson (MHA) (Refs. 1–3) model, associated with the impurity band, has been observed as a function of impurity concentration in doped semiconductors such as doped Si, Ge, GaAs, CdS and others. In these systems, e.g., n -type semiconductors, donor impurities are distributed at random usually occupying substitutional sites. It has been well established experimentally that doped semiconductors undergo a MNM transition beyond a certain impurity concentration N_c . Although doped semiconductors have been widely studied both theoretically and experimentally, the nature of this transition is still not completely elucidated.^{2–14} Mott¹⁵ suggested that the zero-temperature conductivity jumps from zero in the insulator to a certain minimum metallic conductivity value. Furthermore, the scaling theory of localization⁴ showed that around the critical region the MNM transition should be continuous, in contradiction to the existing data that support Mott's original ideas and recent survey.¹⁶

Recently, a high-resolution zero-temperature study of the MNM transition in phosphorus-doped silicon (Si:P), obtained by a uniaxial compressive stress, found a sharp, but nearly continuous MNM transition.⁷ These results seem to differ from both predictions cited above. In even more recent work Kaveh and Mott¹⁴ argue for a qualitative difference between this transition in compensated and uncompensated materials.

The experimental results^{2,3,17} on electrical conduction, susceptibility, specific heat, as well as theoretical investigations^{2,3,10,11,15,18–22} suggest that the MHA model properly describes the novel behavior of a doped semiconductor near the transition. In this model the electron correlation and the Anderson localization are regarded as the most essential factors, and the impurity density of states

(IDS) is split into two Hubbard bands, situated within the band gap of the host material. The lower band consists of D^0 states (related to singly occupied impurities), and the upper band consists of D^- states (doubly occupied impurities). These two bands are separated by the intra-atomic Coulomb correlation energy U . There is direct evidence of this separation in n -type Si and Ge from submillimeter absorption^{3,23} and photoconductivity^{3,24,25} measurements. The correlation effect is seen in the D^- state through the formation of stable bound states, found experimentally by Narita and co-workers,²⁵ and investigated by Kamimura^{2,3,12,26} in a many-valley semiconductor. As the concentration increases the Hubbard bands are broadened and eventually start overlapping each other as well as with the host conduction band (HCB). In essence, it appears that the role of the HCB in the phenomenon of MNM transitions is important primarily in the sense that it serves to determine the form of the cluster distribution of the (localized to extended) impurity states, as we will see later. In addition, recent work^{18,27} has shown that the calculated value of the constant in Mott's condition $N_c^{1/3} a_H^* = \text{const}$ (Refs. 1 and 2) (a_H^* being the effective Bohr radius of the donor electron) is subject to the vagaries of the choice of electronic wave function, as well as being sensitive to the form of the HCB. The influence of the host characteristics, such as the existence of a conduction band with a many-valley character, is believed to be of central importance in the behavior of the physical properties and has been the subject of many recent investigations.^{8,12,18,19,26–36} This inference does not apply to direct-gap semiconductors which have an isotropic conduction band (e.g., GaAs and CdS), and the isolated donor problem is thus just that of a hydrogen atom. On the other hand, in indirect-gap semiconductors (e.g., Si and Ge) the donor electron wave function is a sum over terms which are products of a rapidly oscillating Bloch wave with a hydrogenic envelope which satisfies an effective-mass Schrödinger equation. In silicon, there are six valleys in the HCB at $\vec{k} \neq 0$, and thus the $1s$ ground state of an isolated donor has sixfold degeneracy in the framework of this effective-mass approximation.

Work to date has concentrated much effort in investigating cluster states which provide a great deal of interest in doped semiconductors, particularly the Si:P system, which is a good system for, e.g., Raman studies, since it has the many-valley HCB necessary for a large electronic Raman cross section,²⁹ as well as for electron spin resonance (ESR),³⁷ photoconductivity,^{24,25} and far-infrared absorption spectra³⁸ measurements, where cluster states have appeared in a dominant role. In the light of these investigations, some cluster approaches³⁹⁻⁴² appeared in the literature, particularly those that take into account the many-valley character of the HCB.^{28,31-33,35,43} Recently, the present authors,⁴³ by employing a simple one-electron Hamiltonian (for a one-band model), calculated the IDS of n -type many-valley semiconductors and found it to have a structure different from that of the corresponding one-valley system. Franzén and Berggren,³⁵ in the wake of the cluster model used by Kummer *et al.*⁴⁴ and Walstedt *et al.*⁴² to study the susceptibility of CdS:In, using a Heisenberg Hamiltonian, calculated the magnetic susceptibility and specific heat in the low concentration region, well below N_c , found good agreement with experimental results in Si:P. For the exchange interaction, they used the Kohn-Luttinger (KL) (Ref. 45) wave functions because of the many-valley semiconductors in Si. Their model is also closely related to previous work by Marko and Quirt⁴⁶ and Marko *et al.*⁴⁶ Takemori⁴⁷ and Takemori and Kamimura⁴⁸ with a Gaussian model calculated the magnetic susceptibility and the specific heat reproducing fairly well the characteristic features observed in experiments in Si:P for $1.7 \times 10^{18} \text{ cm}^{-3}$. For the specific heat, they have taken into account the many-valley effects of Si by multiplying by a factor of 6, in the final results, corresponding to the degeneracy.

Searching for a mechanism which would enable us to take into account the degeneracy of the indirect-gap semiconductors, and its influence on the impurity cluster states in the low to intermediate n -type doping regime, i.e., $10^{16} \lesssim N \lesssim 2 \times 10^{17}$ and $2 \times 10^{17} \lesssim N \lesssim 4 \times 10^{18} \text{ cm}^{-3}$, respectively, in Si:P,³² we have performed an improved unrestricted Hartree-Fock-Roothaan (HFR) cluster calculation with such degeneracy effects. In Sec. II we discuss how the many valleys are introduced in the calculation. In Sec. III we present our calculation for the IDS. Section IV is devoted to the investigation of the cluster states to compare them with other investigations and draw some conclusions from our results.

II. MANY-VALLEY UNRESTRICTED HFR APPROACH

For a given impurity concentration N , M random impurity sites $\{\vec{R}_i; i=1, M\}$ are generated with a computer within a volume Ω of a diamond lattice host representing the location of M substitutional impurities, in order to simulate a sample of a doped semiconductor with $N=M/\Omega$. Surrounding these M impurities, additional M_s impurities were similarly generated, in such a way as to keep the impurity concentration unchanged. These M_s impurities will reduce the surface effects and will provide a mean field.^{22,40} With each impurity in Ω is associated a Kohn-Luttinger^{28,32,33,35,43,45} donor wave function

$$\psi_i(\vec{r}) = \frac{1}{\sqrt{\nu}} \sum_{l=1}^{\nu} F_l(\vec{r}) \phi_l(\vec{r}), \quad (1)$$

where $\phi_l(\vec{r})$ is the Bloch function associated with the l th of the ν conduction-band minima of the host material ($\nu=6$ for silicon), and $F_l(\vec{r})$ is a hydrogenic envelope function in which the effective mass at each of these minima has been assumed to be isotropic. Thus the calculation is simplified, since the envelope function can be written as

$$F_l(\vec{r}) = (\pi a_H^*)^{1/3} \exp(-r/a_H^*). \quad (2)$$

The Hamiltonian of the many-electron system is

$$H = \sum_i \frac{p_i^2}{2m} + \sum_i V^{\text{ion}}(\vec{r}_i) + \frac{1}{2} \sum_{i,j} V^{\text{el-el}}(\vec{r}_i - \vec{r}_j), \quad (3)$$

where $V^{\text{ion}}(\vec{r}_i)$ is the impurity-ion potential acting on the i th electron, $V^{\text{el-el}}(\vec{r}_i - \vec{r}_j)$ is the Coulomb interaction between the i th and j th electron, and the summations are over all the M electrons in the volume Ω . This inner cluster will be solved numerically using an unrestricted HFR formalism with spin-polarized potential. This formalism⁴⁹ turns out to be similar to the Hartree-Fock theory used in previous calculations.^{22,41,42} Accordingly, the following two sets of coupled Schrödinger equations arise:

$$\mathcal{H}_\sigma(\vec{r}) \Psi_{n\sigma}(\vec{r}) = E_{n\sigma} \Psi_{n\sigma}(\vec{r}), \quad \sigma = \uparrow, \downarrow \quad \text{and} \quad n = 1, M \quad (4)$$

where

$$\mathcal{H}_\sigma(\vec{r}) = \frac{p^2}{2m} + V^{\text{ion}}(\vec{r}) + V^C(\vec{r}) + V_\sigma^{\text{ex}}(\vec{r}), \quad (5)$$

$V^C(\vec{r})$ is the Coulomb potential, and $V_\sigma^{\text{ex}}(\vec{r})$ is the spin-dependent exchange potential. Taking $\Gamma(\sigma)$ as a set of indices which specifies the $M(\sigma)$ single-particle wave functions that are occupied by σ -spin electrons, the Coulomb and exchange potentials can be expressed as

$$V^C(\vec{r}) = \sum_s \sum_{m \in \Gamma(s)} \int |\Psi_{ms}(\vec{r}')|^2 V^{\text{el-el}}(\vec{r} - \vec{r}') d\vec{r}', \quad s = \sigma, -\sigma \quad (6)$$

and

$$V_\sigma^{\text{ex}}(\vec{r}) \Psi_{n\sigma}(\vec{r}) = - \sum_s \sum_{m \in \Gamma(s)} \delta_{s\sigma} \int \Psi_{ms}^*(\vec{r}') V^{\text{el-el}}(\vec{r} - \vec{r}') \Psi_{n\sigma}(\vec{r}') \times \Psi_{ms}(\vec{r}) d\vec{r}'. \quad (7)$$

The eigenstates of Eq. (4) can be expressed as

$$\Psi_{n\sigma}(\vec{r}) = \sum_j \psi_j(\vec{r}) B_{jn\sigma}, \quad (8)$$

where $\psi_j(\vec{r})$ are given by Eq. (1).

Following the usual HFR procedure, we obtain

$$\sum_j [\bar{B}_\sigma^\dagger \mathcal{H}'_\sigma \bar{B}_\sigma]_{ij} - E_m \delta_{ij} C_{mj\sigma} = 0, \quad (9)$$

where the matrix elements of \mathcal{H}'_σ , are given by

$$\begin{aligned} \mathcal{H}'_{ij\sigma} = & \int \psi_i^*(\vec{r}) \left[\frac{p^2}{2m} + V^{\text{ion}}(\vec{r}) \right] \psi_j(\vec{r}) d\vec{r} \\ & + \sum_{\mu\lambda} \sum_s P_{\mu\lambda}^s \int \int \psi_i^*(\vec{r}) \psi_\mu^*(\vec{r}') V^{\text{el-el}}(\vec{r}-\vec{r}') \\ & \quad \times [\psi_\lambda(\vec{r}') \psi_j(\vec{r}) \\ & \quad - \psi_\lambda(\vec{r}) \psi_j(\vec{r}') \delta_{s\sigma}] d\vec{r} d\vec{r}' \end{aligned} \quad (10)$$

and

$$P_{\mu\lambda}^s = \sum_{m \in \Gamma(s)} B_{\mu ms}^* B_{\lambda ms} \quad (11)$$

To obtain the self-consistent solutions of Eqs. (9) and (10), we first neglect the exchange term in (5) to obtain the Hartree eigensolution \bar{B}_σ . Then we use this \bar{B}_σ as the initial input to obtain $\bar{\mathcal{H}}'_\sigma$, and the corresponding eigenvectors. Once we know $\bar{\mathcal{H}}'_\sigma$ we solve (9) for a new input \bar{B}_σ in order to construct a new $\bar{\mathcal{H}}'_\sigma$ from (10). The numerical interaction continues until a self-consistent solution is reached. Neglecting the three- and four-center integrals, the diagonal and off-diagonal matrix elements of (10) are written explicitly in terms of the Slater integrals^{32,35,50}

$$\begin{aligned} \mathcal{H}'_{ii\sigma} = & E_d + \sum_{k \neq i} J(\vec{R}_{ik}) + UP_{ii}^{-\sigma} + 2 \sum_{k \neq i} P_{ij}^{-\sigma} L(\vec{R}_{ik}) \\ & + \sum_{s=\sigma, -\sigma} \sum_{k \neq i} P_{kk}^s J'(\vec{R}_{ik}) - \sum_{k \neq i} P_{kk}^\sigma K'(\vec{R}_{ik}), \end{aligned} \quad (12)$$

$$\begin{aligned} \mathcal{H}'_{ij\sigma} = & E_d S(\vec{R}_{ij}) + K(\vec{R}_{ij}) + (P_{ii}^{-\sigma} + P_{jj}^{-\sigma}) L(\vec{R}_{ij}) \\ & + \sum_{s=\sigma, -\sigma} P_{ij}^s K'(\vec{R}_{ij}) - P_{ij}^\sigma J'(\vec{R}_{ij}), \end{aligned} \quad (13)$$

where E_d is the ground-state level of an isolated impurity, in units of V_0 , which is equal to twice the ionization energy of the material. Some of these Slater integrals are multiplied by an interference factor, denoted here by I , derived from the many-valley character of the HCB, which is assumed as a valley-symmetric wave function. It is obtained as⁴³

$$I = \frac{1}{\nu} \sum_{l=1}^{\nu} \exp(i \vec{k}_l \cdot \vec{R}), \quad (14)$$

and the integrals are written as follows. The overlap integral is given by

$$S(\vec{R}_{ij}) = S(R_{ij}) I, \quad (15)$$

the energy for the transfer of electrons between impurity sites is

$$K(\vec{R}_{ij}) = V(\vec{R}_{ij}) = V(R_{ij}) I, \quad (16)$$

the electron correlation is

$$L(\vec{R}_{ij}) = L(R_{ij}) I, \quad (17)$$

and the exchange is

$$K'(\vec{R}_{ij}) = K'(R_{ij}) I^2. \quad (18)$$

The expressions $J(\vec{R}_{ik})$ and $J'(\vec{R}_{ij})$ remain unaltered, the vector $\vec{R} = \vec{R}_i - \vec{R}_j = \vec{R}_{ij}$ corresponds to the separation of a pair of donor impurity centers at sites \vec{R}_i and \vec{R}_j , and the vectors $\vec{k}_l = \pm k\hat{x}$, $\pm k\hat{y}$, $\pm k\hat{z}$ represent the values of the Bloch wave vectors at the conduction-band minima for silicon in three mutually perpendicular $\langle 100 \rangle$ directions. Spectroscopic experiment has lead Dumke⁵¹ to localize the minima at $2\pi/a(0.82, 0, 0)$, i.e., at about 82% of the distance to the Brillouin-zone boundary, and equivalent points, where a is the lattice parameter of Si. Accordingly, the length of the vector \vec{k}_l is $|\vec{k}_l| = 0.82(2\pi/a) = 16.41$, where $a_H^* = 17.3$ Å, the Bohr radius of Si:P, and $a = 5.42$ Å were used. As a consequence of the valleys in Si, Eqs. (15)–(18) have an oscillatory behavior as shown in Figs. 1 and 2, which will reduce the broadening of the IDS. Neglecting the valleys, Eq. (1) must be substituted by Eq. (2). No adjustable parameters whatsoever have been used other than the above well-known values. We have used the value of a_H^* as determined from an ESR investigation by Cullis and Marko²⁸ who used the KL wave function to calculate the donor-pair exchange energy, and included the conduction-band degeneracy. The term U remains unaltered at $\frac{5}{8}$ (effective hartree). We also use the corresponding experimental value $U/V_0 = 0.475$ to calculate the density of states. The D^0 band remains unaltered while the center of gravity of the D^- band, at very low concentration, is lowered to a value of -0.0275 effective hartree which is consistent with experimental results.²⁵ With the use of a Chandrasekhar⁵² wave function, conveniently parametrized, for the D^- orbital, Riklund and Chao⁴² found a value consistent with experiment and calculated the impurity states, which will be compared with our calculation.

III. IDS

The IDS $D(E)$ is normalized to

$$\int D(E) dE = \frac{p}{32\pi} = (M/\Omega) a_H^{*3}, \quad (19)$$

where p is defined as a dimensionless impurity concentration $p = 32\pi M a_H^{*3} / \Omega$. For Si:P the critical concentration is around $p_c \simeq 2.0$, taking $a_H^* = 17.3$ Å⁰ and $N_c = 3.74 \times 10^{18}$ cm⁻³ (Ref. 5). In our calculation we use inner clusters of $M = 40$ impurities, 960 outer impurities, and a configuration average over 50 samples. The Fermi energy is obtained through

$$\int_{-\infty}^{E_F} D(E) dE = \frac{M \times LS}{\Omega} a_H^{*3}, \quad (20)$$

at 0 K. Of course, E_F was assumed to be the same in the whole sample, that is, in each of the LS configurations. This should be checked with the assumption made in the HFR calculations, namely, that the first M states of low energy were occupied in each configuration. When this condition is not satisfied, we expect an internal charge transfer between different configurations, and the HFR calculations would have to be performed accordingly. This “charge inhomogeneity” generation can, in some aspects, be compared to the self-compensation effects in early work,³¹ and could play a similar role in the physical

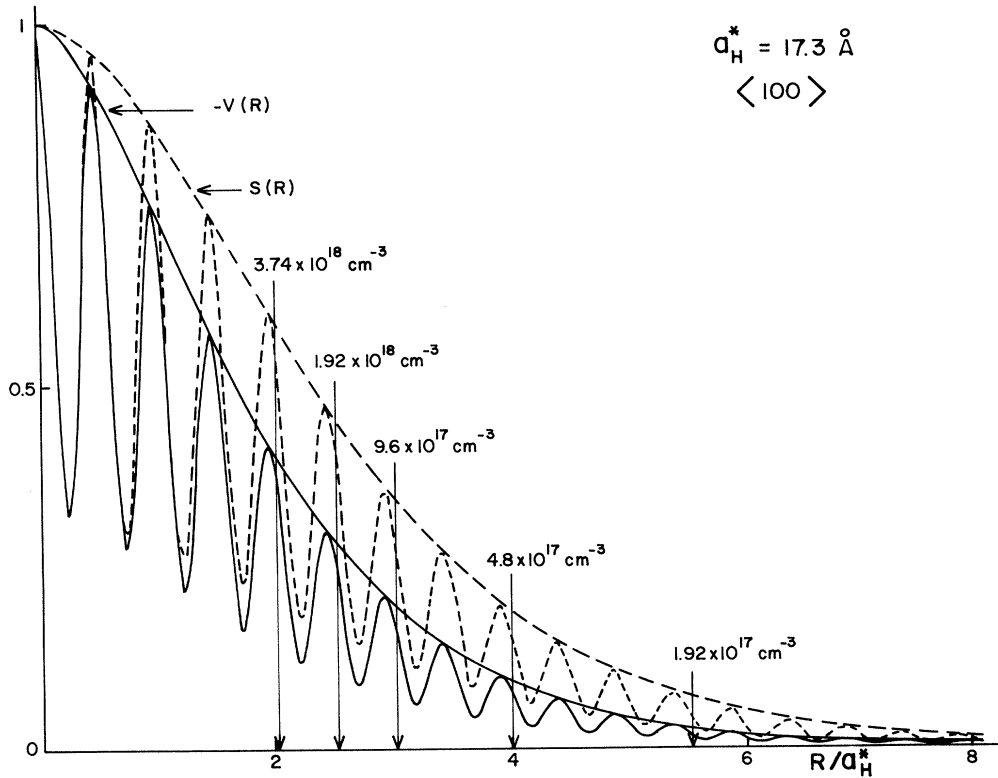


FIG. 1. Effective overlap $S(R)$ and electron-hopping energy $V(R)$ integrals as a function of distance R between impurity centers in Si. The dashed and solid wiggly curves refer to anisotropic equations [(15) and (16)]. The dashed and solid straight curves refer to the case of neglecting the oscillatory factor deriving from the many-valley character of the HCB. The latter case is relevant to, for example, *n*-type CdS and GaAs. The vector \vec{R} between the two impurity centers is in the $\langle 100 \rangle$ direction. The arrows indicate the mean separation of donors at different concentrations. The effective Bohr radius used was $a_H^* = 17.3 \text{ \AA}$. The impurity critical concentration for MNM transition in Si:P is $3.74 \times 10^{18} \text{ cm}^{-3}$.

properties. We will call it “inner compensation”, stressing the fact that it is not caused by structural defects or strange impurities, but only by the potential fluctuation of the system itself. This effect causes in fact a serious limitation in the cluster approach, since it would be very time consuming and expensive to incorporate it self-consistently in the HFR calculations. Fortunately, and this is a significant result, the incorporation of the many-valley character of the host causes it to be much reduced in indirect-gap semiconductors, such as Si or Ge. For an estimate of this effect, we simply discarded the configurations whose occupations did not conform with the Fermi energy calculated from Eq. (20). Then E_F is recalculated again and, in the final sample, we keep the fraction f of initial configurations, which are consistent with Eq. (20). With the KL basis functions, the fraction f ranges from 1, on low concentrations, to more than 0.9 for $p = 1.0$, compared to the value of 0.5 obtained for $p = 1.0$ with the simple $1s$ wave function. In Fig. 3 we show the IDS for $p = 0.5$ (corresponding to $N = 9.6 \times 10^{17} \text{ cm}^{-3}$ of Si:P) from two different clusters calculations. In the histogram 3(a) there is no inner-compensation effect during the self-consistency, while the histogram 3(b) was obtained by the selected configurations consistent with Eq. (20), such that no configuration has an occupation less than $M/2$ or greater than $3M/2$ (we found that the HFR levels are not too sensitive in this range). For the latter case [histogram

3(b)], the impurity states are rather sensitive; the overall IDS will be enhanced, the high-energy tail of the lower Hubbard band shifts down considerably, and the upper band remains approximately unaltered and the Fermi energy (E_F) and $D(E_F)$ will be lowered and raised, respectively. Apart from the HFP limitation and the cluster size, certainly the inner compensation is very important for higher concentrations, but its effect is greatly reduced by the inclusion of the oscillatory behavior of the wave functions due to the HCB minima. In what follows we will carry out the calculation with the correction discussed above.

The IDS obtained are shown in Figs. 4 and 5 as a function of impurity concentration $p = 0.25$ and 1.0 (corresponding to 4.8×10^{17} and $1.92 \times 10^{18} \text{ cm}^{-3}$, respectively, for Si:P). The histograms 4(a) and 5(a) are obtained by neglecting the oscillatory factor deriving from the many-valley character of the HCB, while the histograms 4(b) and 5(b) take this into account. The bandwidths are much reduced, the $D(E)$ increases, and the E_F decreases by including degeneracy. The g ratio defined by Mott as a measure of the strength of the pseudogap will gradually diminish. The E_F is plotted in Fig. 6 for different situations showing its sensitivity of the choice of the calculation. When the E_F passes the HCB, a critical concentration $N_{cb} \gg N_c$ is assumed.⁵³ It was suggested that this transition results from the fact that the impurity is im-

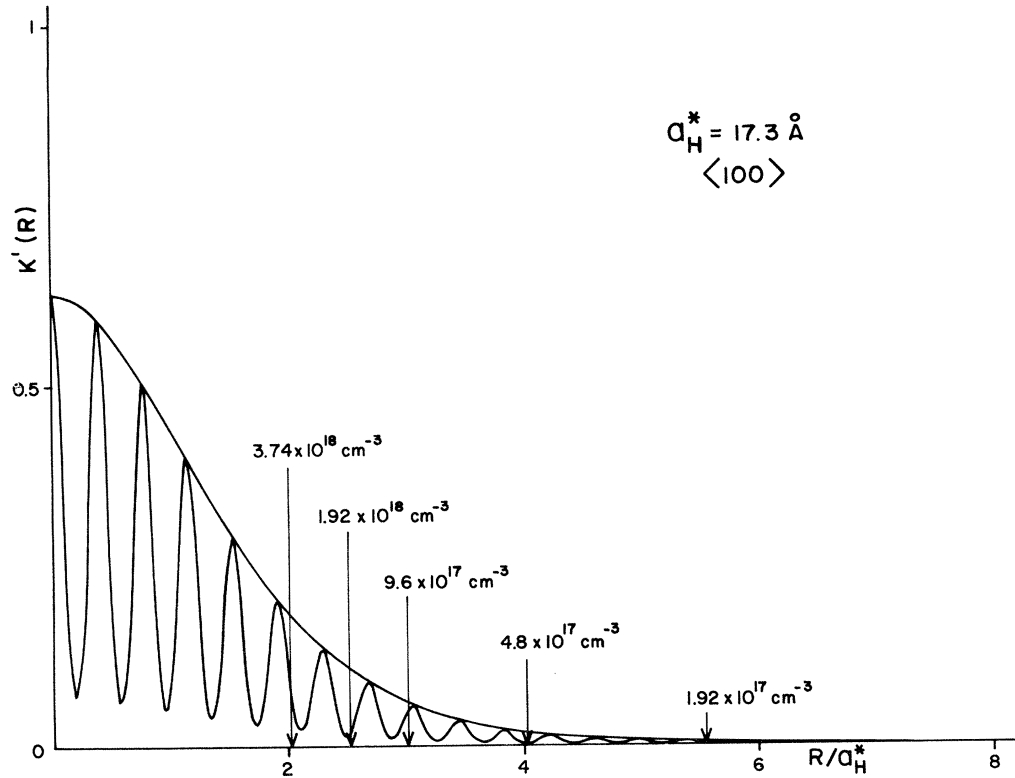


FIG. 2. Same as Fig. 1, for the effective exchange interaction $K'(R)$, Eq. (18), as a function of distance R between impurity centers in Si.

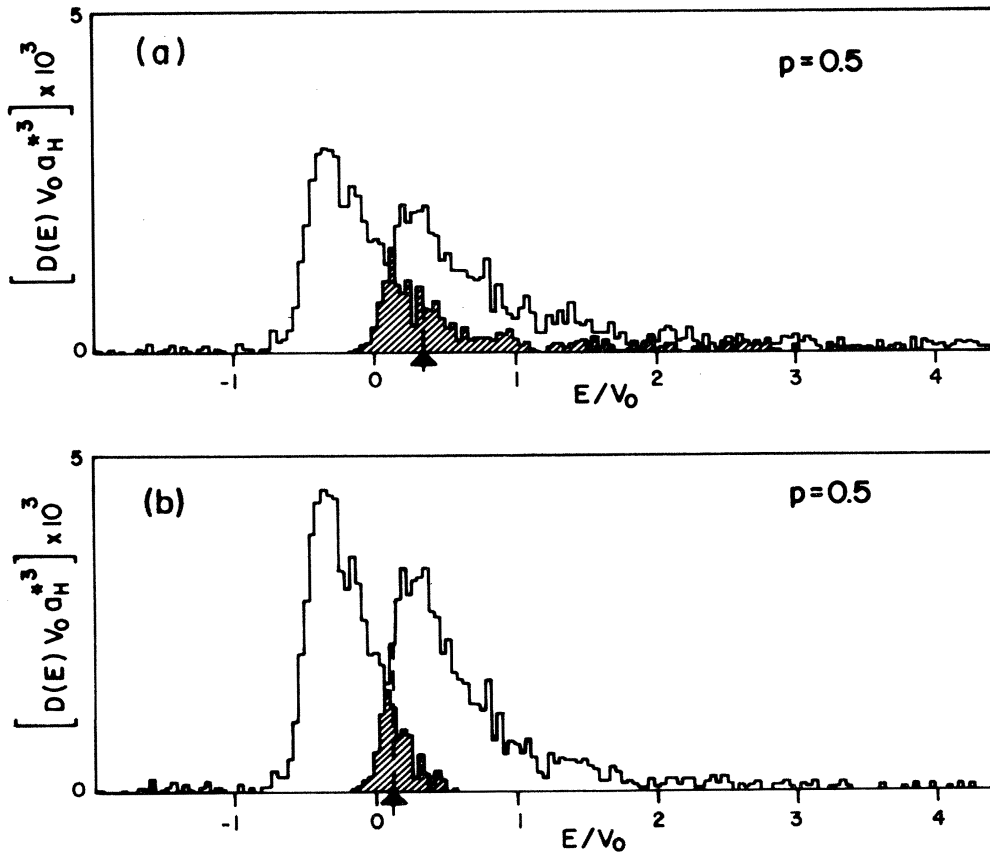


FIG. 3. IDS calculated without and with (b) inner compensation for $p = 0.5$. The arrow indicates E_F .

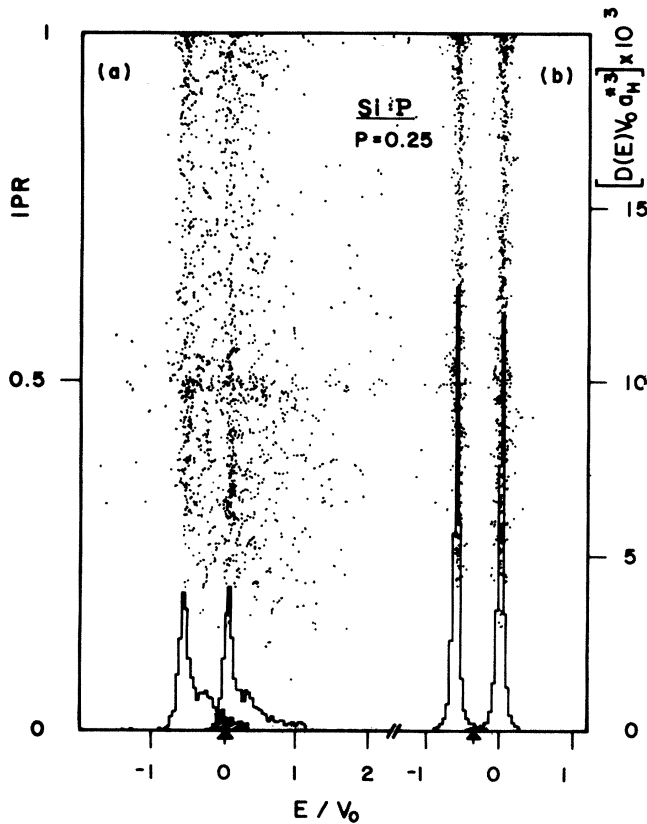


FIG. 4. IDS without (a) and with (b) many-valley character of the Si HCB. The HCB is set at zero energy. Shaded area represents the overlap of split bands. The dots correspond to the IPR, and $p=0.25$ corresponds to $4.8 \times 10^{17} \text{ cm}^{-3}$, for Si:P, $a_H^* = 17.3 \text{ \AA}$. The arrow indicates E_F .

mersed in a host matrix holding it together, for Si:P, $N_{cb} = 2.0 \times 10^{19} \text{ cm}^{-3}$, corresponding to $p \approx 10$. In Fig. 6 we show the change in E_F with concentration obtained from these cluster calculations with various models. In fact, the calculations with the single hydrogenoid model yields a IDS with dispersion that is too large for concentrations, even below the MNM transition, and the value of E_F cannot be located with reasonable reliability.^{39,40} The curves in Fig. 6 show that the inner-compensation effect has a considerable influence in the location of E_F , and that the single hydrogenoid model for the atomic state of the donor impurity does not reproduce, even qualitatively, the experimental behavior. The inclusion of the KL wave functions gives the right behavior of E_F , and reduces the bandwidth and the dispersion in the IDS. The location of E_F is fairly realistic in the range of concentrations considered here.

IV. IMPURITY CLUSTER STATES AND DISCUSSION

In order to have a microscopic view of the IDS, we have used the inverse participation ratio (IPR) and a probability distribution of cluster states. The IPR that has been used in earlier numerical calculations^{42,43,54} as a measure of localization of the eigenstate has been defined as

$$\mathcal{R}_{IPR n \sigma} = \left[\sum_{j=1}^M |B_{jn\sigma}|^4 \right] / \left[\sum_{j=1}^M |B_{jn\sigma}|^2 \right]^2 \quad (21)$$

(where \mathcal{R}_{IPR} is the IPR), for the n th eigenstate with spin σ , where $B_{jn\sigma}$ comes from (8). The IPR, dots appearing on Figs. 4 and 5, varies from 1, corresponding to a state which is as localized as possible, to $1/M$, corresponding to a state which is as extended as possible. In Figs. 4(a) and 5(a) the IPR is obtained by neglecting the many-valley effects of the HCB, while for Figs. 4(b) and 5(b) these effects are taken into account. For low concentration, most of the states have an IPR between 0.5 and 1.0 indicating an isolated impurity state or a pair state. Going to intermediate regions approaching N_c , where large clusters become more probable than isolated close pairs, the IPR for case (b) delocalizes less rapidly than for case (a), indicating a shift in the energy of the delocalized conducting states. Even for such higher concentrations, some of the occupied states will be localized, which is supported by the absorption measurements on doped silicon by Schmid,⁵⁵ who also theoretically estimated the band-gap narrowing using arguments rather similar to the work of Berggren and Sernelius,³⁴ and the calculation on direct-gap GaAs by Serre *et al.*,⁵⁶ who focused attention on the relative of multiple-impurity scattering and impurity-concentration fluctuation, obtaining a band tailing. In a recent paper of Sernelius,³⁶ where the ion potentials are approximated by pure Coulomb potentials and the donor electrons are treated as an electron liquid surrounding the impurity ions, the high-stress optical birefringence and piezoresistance were investigated in heavily doped many-valley germanium. This calculation is carried out including the number of valleys ($\nu=4$), the effective mass, and a screening constant, and it shows that the band-tailing effects are reduced when the many-valley character of the HCB is taken into account. Now, taking the mean value of the IPR for each sample of the cluster, at a fixed concentration, and also the configuration average of the IPR ($\langle IPR \rangle$) over all the sample clusters as shown in Fig. 7, we can see that in case (a) no valley effect, the $\langle IPR \rangle$ for $p < 0.3$ (corresponding to $N < 5.76 \times 10^{17} \text{ cm}^{-3}$ for Si:P), is greater than 0.5, while for case (b), with valley effect, only for $p < 0.8$ ($N < 1.92 \times 10^{18} \text{ cm}^{-3}$) the $\langle IPR \rangle$ is greater than 0.5. Calculating the magnetic susceptibility by a modified pair approximation including many-valley effects Andres *et al.*³³ showed that their results agree well with the experimental data up to concentration around $1.2 \times 10^{18} \text{ cm}^{-3}$ ($p \approx 0.6$) for P-doped Si, which shows that the system is composed by isolated impurities or pairs of impurities. With increasing impurity concentration, higher density fluctuations will be present and the probability of having cluster states covering a number of impurities is shown in Fig. 8. In Fig. 8(a) the degeneracy of the HCB is neglected and the picture is similar to the results of Riklund and Chao,⁴² but $p = 1.0$ corresponds to $1.92 \times 10^{18} \text{ cm}^{-3}$, below the MNM transition, while considering the many-valley effect, Fig. 8(b), a larger cluster appears around $p \approx 2.0$ where the MNM transition takes place. From Figs. 4(b), 5(b), 7(b), and 8(b) the states turn out to be more extended around $p_c(N_c)$. Our results, outlined above, are also in agreement with the conclusions reached by Thomas *et al.*³² through their analysis of opti-

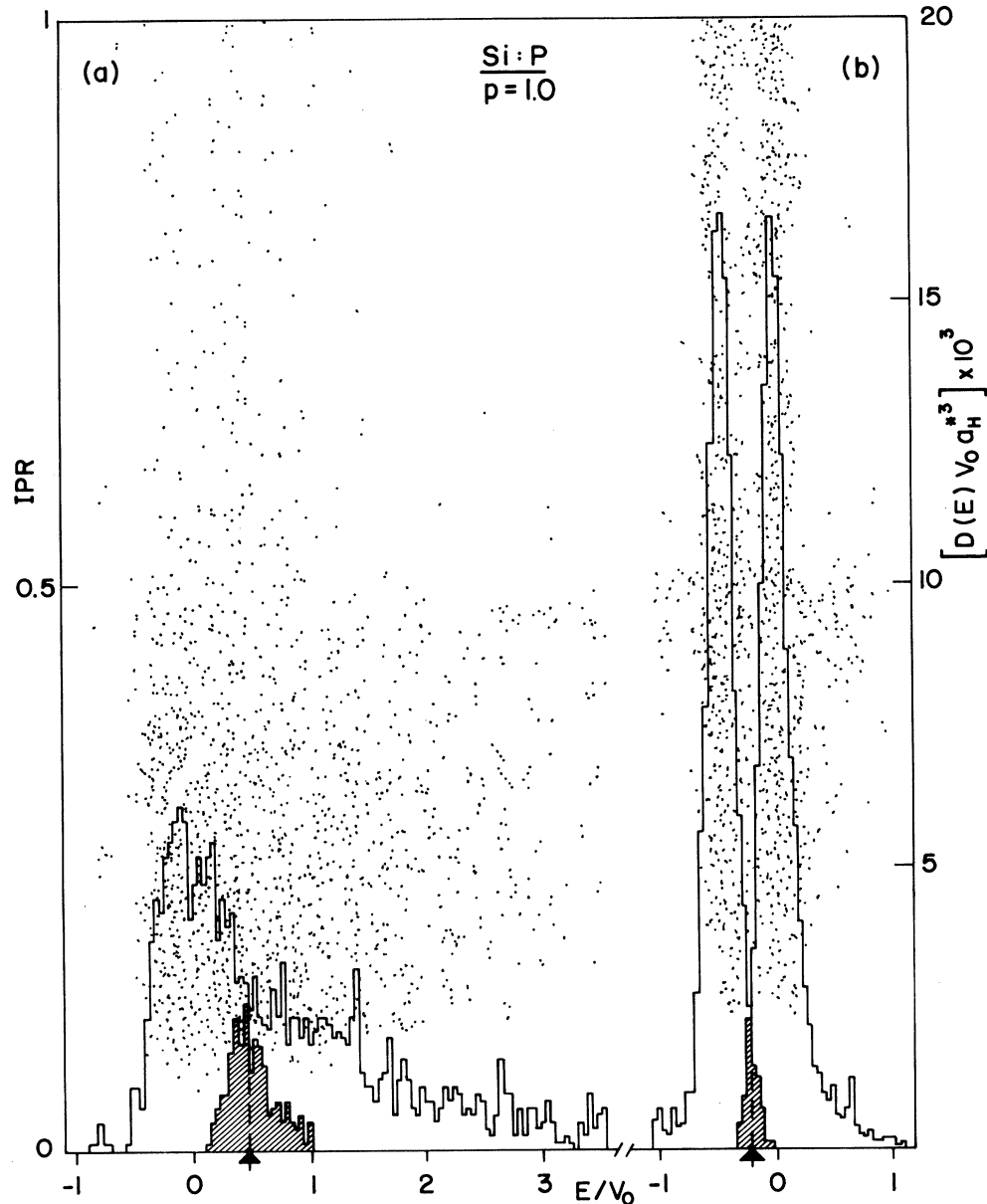


FIG. 5. Same as Fig. 4 for $p = 1.0$, corresponding to $1.92 \times 10^{18} \text{ cm}^{-3}$ for Si:P.

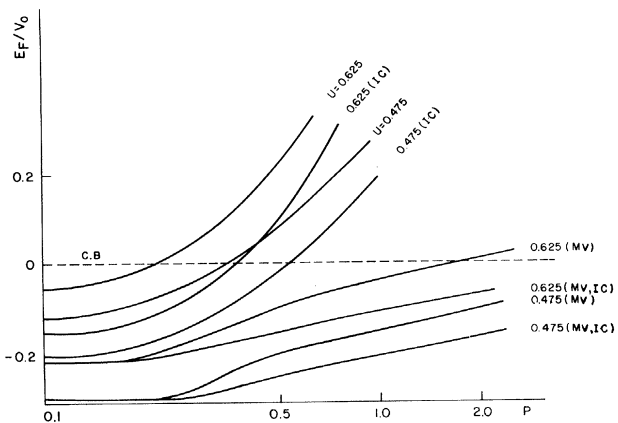


FIG. 6. Fermi energy as a function of the impurity concentration p for different calculations involving the U , many-valley (MV), and inner-compensation (IC) effects.

cal data. Some experimental clues exist also in ESR (Ref. 37) investigation supporting this clustering evidence. For low concentration ($N \lesssim 7.0 \times 10^{17} \text{ cm}^{-3}$, $p \lesssim 0.4$), hyperfine-split ESR lines exist and they are characteristic of electrons bound on donor sites. With increasing impurity concentration until clusters of eight or ten atoms form, this multiple line pattern fades into that of a single unresolved ESR line. For Si:P the delocalization occurs at $N \approx 3.7 \times 10^{18} \text{ cm}^{-3}$ ($p \approx 2.0$). It is worth noting that for the same spatial disorder, the electronic correlation is much affected by the many-valley effect. The overlap, exchange, and the electron-hopping energy integrals on two neighboring donors are much reduced on the average and so is the broadening of the IDS, showing a new feature in the overall impurity states of indirect-gap semiconductors.

The above results should be compared to the work of

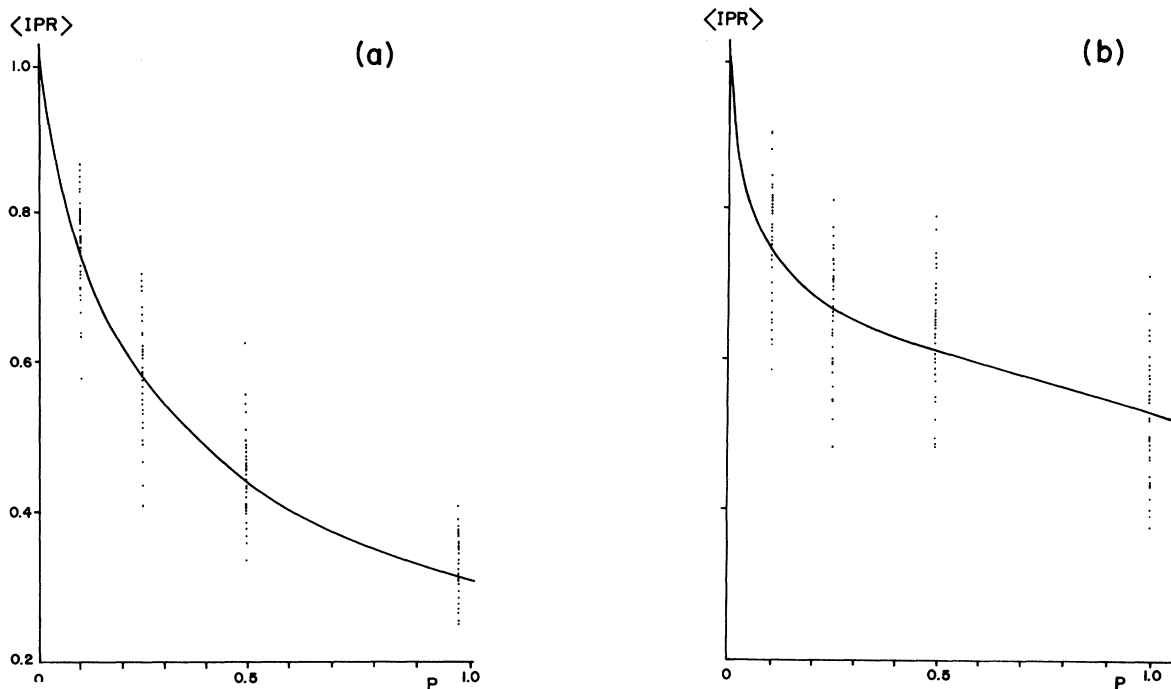


FIG. 7. $\langle IPR \rangle$ for various values of the impurity concentration p . Curve (a) neglects the many-valley character of the HCB. Curve (b) considers such previous effects.

Bhatt and Rice.³¹ In that work, a very interesting calculation is carried out with molecular clusters with a highly degenerate $1s$ atomic state, but not taking into account explicitly the different positions of the minima in reciprocal

space. Within this approximation, these authors found that large clusters in multivalley semiconductors can attract electrons from isolated donors on donor pairs, and so correlation effects do not impose the location of the Fermi

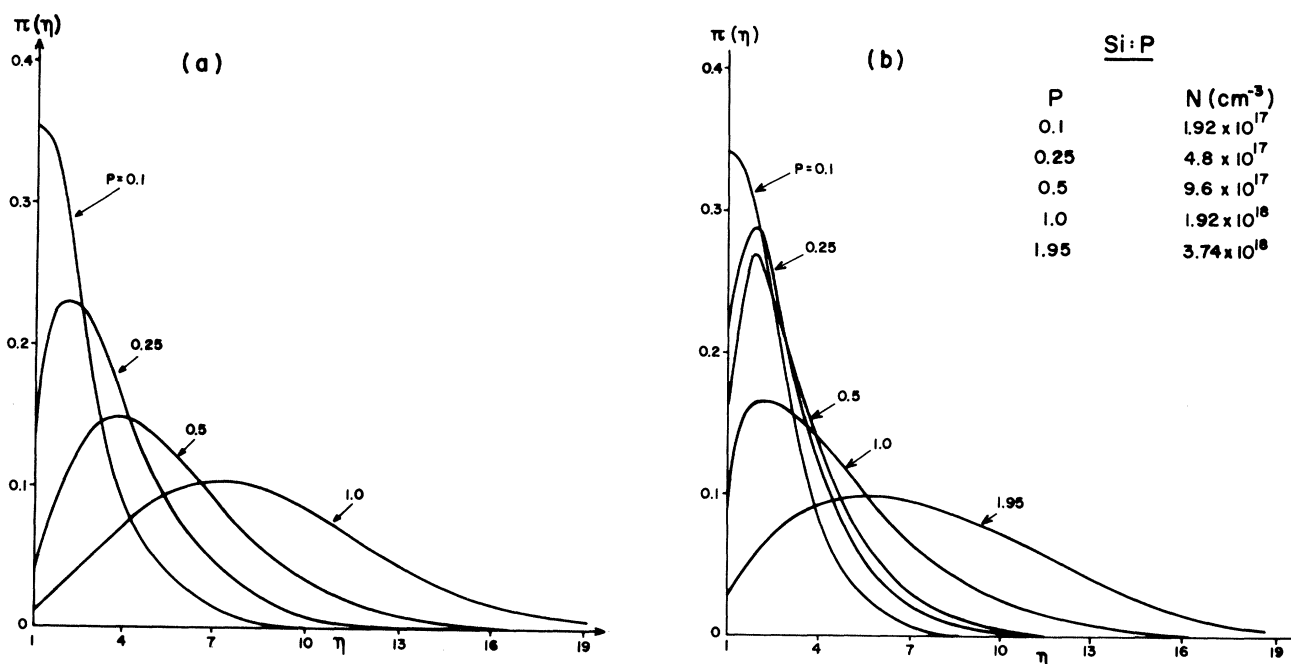


FIG. 8. (a) Probability distribution of cluster as a function of the number of impurities covered by the cluster states, for various values of the impurity concentrations p (or N). (b) Same as 8(a), but considering the many-valley character of the Si HCB.

energy in a Coulomb gap. We think that, at this stage, it would be interesting to carry out more detailed calculations with the use of an extended orbital basis of the Kohn-Luttinger type. This calculation could be carried out either by our rather detailed HFR approach or by the density-functional method employed by Bhatt and Rice.³¹ It is to be noted that, according to the approximations that led to Eqs. (15)–(18), the Coulomb and exchange interactions would be affected quite differently, and therefore the question of the existence of a Coulomb gap at the Fermi energy must be examined more carefully.

Finally, we point out that the measure of localization we adopted here, namely, the IPR, as defined by Eq. (21), should be compared with some care with the localization in real space. A molecular state that covers N sites equal-

ly would have an IPR of $1/N$; for $N \approx 5$, the IPR is as small as 0.2, and this can be of little information about localization in coordinate space, unless we know where the sites are. The pertinent point is that, according to the curves of Figure 8, the cluster states that we observed are almost all very small compared with the cluster size, and so we expect that a host of physical properties, that do not depend strongly on the localization in real space, can be clarified by these simulations. In particular, the corrections in the basis functions of a donor impurity for indirect-gap semiconductors, that was the main purpose of the present investigation, was proved to be essential for the explanation of almost all the electronic properties of these systems.

- ¹N. F. Mott, *Metal-Insulator Transitions* (Taylor and Francis, London, 1974).
- ²*The Metal-Insulator Transition in Disordered Systems*, edited by L. R. Friedman and D. P. Tunstall (Scottish Universities Summer School in Physics, Edinburgh, 1978).
- ³Proceedings of the International Conference on Impurity Bands in Semiconductors, Würzburg, West Germany, 1979, edited by M. Von Ortenberg, [Philos. Mag. B **42**, (1980)].
- ⁴E. Abrahams, P. W. Anderson, D. C. Licciardello, and T. V. Ramakrishnan, Phys. Rev. Lett. **42**, 673 (1979).
- ⁵T. F. Rosenbaum, K. Andres, G. A. Thomas, and R. N. Bhatt, Phys. Rev. Lett. **45**, 1723 (1980).
- ⁶G. A. Thomas, Y. Ootuka, S. Kobayashi, and W. Sasaki, Phys. Rev. B **24**, 4886 (1981); G. A. Thomas, Y. Ootuka, S. Katsumoto, S. Kobayashi, and W. Sasaki, *ibid.* **25**, 4288 (1982).
- ⁷M. A. Paalanen, T. F. Rosenbaum, G. A. Thomas, and R. N. Bhatt, Phys. Rev. Lett. **48**, 1284 (1982).
- ⁸K.-F. Berggren, J. Phys. C **15**, L45 (1982).
- ⁹K.-F. Berggren, in *The Metal-Insulator Transition in Disordered Systems*, Ref. 2, p. 399; (private communication).
- ¹⁰Proceedings of the 1st Brazilian School on the Physics of Semiconductors, Campinas 1983, Brazil [Rev. Bras. Física (special issue)].
- ¹¹H. Kamimura, in *Proceedings of the 1st Brazilian School on the Physics of Semiconductors* Ref. 10, p. 185; (private communication).
- ¹²H. Kamimura, in *Modern Problems in Condensed Matter Sciences*, edited by M. Pollack and A. L. Efros, (North-Holland, Amsterdam, to be published).
- ¹³K.-F. Berggren, in proceedings of the 1st Brazilian School on the Physics of Semiconductors, Ref. 10, p. 221; (private communication).
- ¹⁴M. Kaveh and N. F. Mott, J. Phys. C **15**, L697 (1982); **15**, L707 (1982).
- ¹⁵N. F. Mott, Philos. Mag. **22**, 7 (1970); **26**, 1015 (1972).
- ¹⁶N. F. Mott, Philos. Mag. **44B**, 265 (1981).
- ¹⁷E. A. Davis and W. D. Compton, Phys. Rev. **140**, A2183 (1965); Y. Otsuka, S. Ikihata, S. Kobayashi, and W. Sasaki, Solid State Commun. **20**, 441 (1976); J. D. Quirt and J. R. Marko, Phys. Rev. B **5**, 716 (1972); J. R. Marko, M. P. Harrison, and J. D. Quirt, *ibid.* **10**, 2448 (1974); N. Kobayashi, S. Ikehata, and W. Sasaki, Solid State Commun. **32**, 1147 (1979).
- ¹⁸K.-F. Berggren, Philos. Mag. **27**, 1027 (1973); **30**, 1 (1974).
- ¹⁹B. E. Sernelius and K.-F. Berggren, Philos. Mag. B **43**, 115 (1981); K.-F. Berggren, in *The Metal-Insulator Transition in Disordered Systems*, Ref. 2, p. 399.
- ²⁰H. Aoki and H. Kamimura, J. Phys. Soc. Jpn. **40**, 6 (1976)
- ²¹A. Ferreira da Silva, I. C. da Cunha Lima, and R. Kishore, Phys. Rev. B **23**, 4035 (1981); R. Kishore, I. C. da Cunha Lima, M. Fabbri, and A. Ferreria da Silva, *ibid.* **26**, 1038 (1982); I. C. da Cunha Lima, M. Fabbri, and A. Ferreira da Silva, Phys. Status Solidi B **111**, K69 (1982).
- ²²K. A. Chao, A. Ferreira da Silva, and R. Riklund, Suppl. Prog. Theor. Phys. **72**, 181 (1982).
- ²³K. Yoshihiro, M. Tokumoto, and C. Yamanouchi, J. Phys. Soc. Jpn. **36**, 310 (1974).
- ²⁴P. Norton, Phys. Rev. Lett. **37**, 164 (1976).
- ²⁵M. Taniguchi and S. Narita, Solid State Commun. **20**, 131 (1976); J. Phys. Soc. Jpn. **43**, 1262 (1977); S. Narita and M. Kobayashi, Philos. Mag. B **42**, 895 (1980).
- ²⁶A. Natori and H. Kamimura, J. Phys. Soc. Jpn. **43**, 1270 (1977); H. Kamimura, J. Non-Cryst. Solids **32**, 187 (1979).
- ²⁷F. Martino, G. Lindel, and K.-F. Berggren, Phys. Rev. B **8**, 6030 (1973).
- ²⁸P. R. Cullis and J. R. Marko, Phys. Rev. B **1**, 632 (1970).
- ²⁹K. Jain, S. Lai, and M. V. Klein, Phys. Rev. B **13**, 5448 (1976).
- ³⁰T. G. Castner and H. S. Tan, Phys. Rev. B **23**, 4000 (1981); R. N. Bhatt, *ibid.* **24**, 3630 (1981); **26**, 1082 (1982).
- ³¹R. N. Bhatt and T. M. Rice, Philos. Mag. B **42**, 859 (1980); Phys. Rev. B **23**, 1920 (1981).
- ³²G. A. Thomas, M. Capizzi, F. De Rosa, R. N. Bhatt, and T. M. Rice, Phys. Rev. B **23**, 5472 (1981).
- ³³K. Andres, R. N. Bhatt, P. Goalwin, T. M. Rice, and R. E. Walstedt, Phys. Rev. B **24**, 244 (1981).
- ³⁴K.-F. Berggren and B. E. Sernelius, Phys. Rev. B **24**, 1971 (1981).
- ³⁵N.-I. Franzén and K.-F. Berggren, Philos. Mag. B **23**, 29 (1981); Phys. Rev. B **25**, 1993 (1982); N.-I. Franzén, Philos. Mag. B **27**, 565 (1983).
- ³⁶B. E. Sernelius, Phys. Rev. B **27**, 6234 (1983).
- ³⁷G. Feher, Phys. Rev. **114**, 1219 (1959); S. Maekawa and N. Kinoshita, J. Phys. Soc. Jpn. **20**, 1447 (1965); M. Rosso *ibid.* **38**, 780 (1975); D. F. Holcomb, in *The Metal-Insulator Transition in Disordered Systems*, Ref. 2, p. 251.
- ³⁸K. Nagosaka and S. Narita, Solid State Commun. **7**, 467 (1963); S. Narita, M. Taniguchi, and M. Kobayashi, in *Proceedings of the 14th International Conference on the Physics of Semiconductors, Edinburgh, 1978*, edited by B. L. H.

- Wilson (IOP, Bristol, 1978), p. 989; M. Kobayashi, Y. Sakaida, M. Taniguchi, and S. Narita, *J. Phys. Soc. Jpn.* **47**, 138 (1979).
- ³⁹J. Golka and L. Piela, *Solid State Commun.* **21**, 691 (1977); J. Golka, *Philos. Mag. B* **40**, 513 (1979); M. Capizzi, G. A. Thomas, F. De Rosa, R. N. Bhatt, and T. M. Rice, *Phys. Rev. Lett.* **44**, 1019 (1980); J. Golka and H. Stoll, *Solid State Commun.* **33**, 1183 (1980).
- ⁴⁰A. Ferreira da Silva, R. Riklund, and K. A. Chao, *Prog. Theor. Phys.* **62**, 584 (1979).
- ⁴¹K. A. Chao, R. Riklund, and A. Ferreira da Silva, *Phys. Rev. B* **21**, 5745 (1980); R. Riklund, A. Ferreira da Silva, and K. A. Chao, *Philos. Mag. B* **42**, 755 (1980); M. Fabbri and A. Ferreira da Silva, in *Proceedings of the 1st Brazilian School on the Physics of Semiconductors*, Ref. 10, p. 370.
- ⁴²R. Riklund and K. A. Chao, *Phys. Rev. B* **26**, 2168 (1982).
- ⁴³M. Fabbri and A. Ferreira da Silva, *J. Non-Cryst. Solids* **55**, 103 (1983).
- ⁴⁴P. B. Kummer, R. E. Walstedt, S. Geschwind, V. Narayanamurti, and G. E. Devlin, *Phys. Rev. Lett.* **40**, 1098 (1978); R. E. Walstedt, S. Geschwind, V. Narayanamurti, and G. E. Devlin, *J. Appl. Phys.* **50**, 1700 (1979).
- ⁴⁵W. Kohn and J. M. Luttinger, *Phys. Rev.* **98**, 915 (1955); W. Kohn, in *Solid State Physics*, edited by F. Seitz and D. Turnbull (Academic, New York, 1957), Vol. 5.
- ⁴⁶J. R. Marko and J. D. Quirt, *Phys. Status Solidi B* **64**, 325 (1974); J. R. Marko, J. P. Harrison, and J. D. Quirt, *Phys. Rev. B* **10**, 2448 (1974).
- ⁴⁷T. Takemori, Ph.D. thesis, University of Tokyo, 1983 (unpublished).
- ⁴⁸T. Takemori and H. Kamimura, *J. Phys. C* **16**, 5167 (1983).
- ⁴⁹C. C. J. Roothaan, *Rev. Mod. Phys.* **23**, 69 (1951).
- ⁵⁰J. C. Slater, *Quantum Theory of Molecular and Solids* (McGraw-Hill, New York, 1968), Vol. I, p. 58.
- ⁵¹W. P. Dumke, *Phys. Rev.* **118**, 938 (1960).
- ⁵²S. Chandrasekhar, *Astrophys. J.* **100**, 176 (1974).
- ⁵³M. N. Alexander and D. F. Holcomb, *Rev. Mod. Phys.* **40**, 815 (1968); D. F. Holcomb, in *The Metal-Insulator Transition in Disordered Systems*, Ref. 2, p. 251.
- ⁵⁴W. M. Visscher, *J. Non-Cryst. Solids* **8-10**, 477 (1972); D. C. Licciardello and D. J. Thouless, *J. Phys. C* **11**, 925 (1978).
- ⁵⁵P. E. Schmid, *Phys. Rev. B* **23**, 5531 (1981).
- ⁵⁶J. Serre, A. Ghazali, and P. Leroux Hugon, *Phys. Rev. B* **23**, 1971 (1981).